Optics Letters

Dual-focal waveguide see-through near-eye display with polarization-dependent lenses

Chanhyung Yoo,[1] Kiseung Bang,[1] Changwon Jang,[1] Dongyeon Kim,[1] Chang-Kun Lee,[2] Geeyoung Sung,[2] Hong-Seok Lee,[2] and Byoungho Lee[1,*]

[1]School of Electrical and Computer Engineering, Seoul National University, Gwanak-Gu Gwanakro 1, Seoul 08826, South Korea
[2]Imaging Device Laboratory, Samsung Advanced Institute of Technology, Samsung Electronics, Suwon, Gyeonggi-do 16678, South Korea
*Corresponding author: byoungho@snu.ac.kr

A waveguide near-eye display (NED) with a dual-focal plane using a polarization-dependent lens device is proposed. The novel optical device is composed of a geometric phase holographic lens, a wave plate, and a circular polarizer, which is operating as a concave lens or a see-through optical window, depending on the polarization state of the input beam. Such property and ultra-thinness of about 1.5 mm can be applied to a combiner-eyepiece lens for augmented reality. This optical device attached to the waveguide provides two depth planes with polarization multiplexing. We have demonstrated that our proof-of-concept system has image planes at infinity and 20 diopters. The devised system can be expected to offer a better immersive experience, compared to a NED system with a single-focal plane. © 2019 Optical Society of America

https://doi.org/10.1364/OL.44.001920

A near-eye display (NED), which can offer an immersive virtual experience in real time, has rapidly been developing over the past few years. Today, an augmented reality (AR) NED is being released in the market. Microsoft [1], Google [2], Sony [3], and other related corporations have already launched wearable helmet-mounted or glasses-type display systems. The optical design of the see-through NED can be summarized into two main concepts: the "mirror-based type" and "waveguide-based type." [4]

The mirror-type NED uses a semi-transparent mirror as an optical combiner [5]. This NED system can be implemented with comparatively simple optical devices. However, these systems suffer from bulky form-factors. The second concept using a waveguide technique allows lightweight and compact form-factors. By using a thin waveguide and optical couplers, we can eliminate cumbersome optical components in front of the eye that obstruct the view of the user. This approach may be appropriate to integrate an AR environment in daily life.

In the waveguide-type NED, a collimated light is extracted to the user's eye by an optical coupler on the output part. In this case, virtual images are focused at infinity, and the observer's eye is forced to focus at infinity by an accommodation response.

If a real object is located near a user, augmented images appear blurred due to the difference of accommodation depth between real objects and display images. This problem may hinder the user from vividly experiencing mixed reality and induce the visual fatigue by the mismatch between accommodation and vergence distance, which is called vergence-accommodation conflict (VAC) [6–8].

To mitigate the problem, various solutions have been proposed and are summarized in [9]. Given that most of them have additional bulky optics to adjust the focal plane, they are difficult to directly employ in a waveguide display. Zhan et al. proposed a multi-focal additive light-field display by using switchable Pancharatnam–Berry phase lenses [10]. This method provides multi-focal planes with compact lenses. However, it is inadequate for AR systems due to the exclusion of real-world scene.

In the NED based on a waveguide, other approaches have been proposed. Yeom et al. proposed a waveguide-type holographic NED, which can deliver a holographic image offering a natural accommodation response [11]. The see-through NED based on the holographic principle, however, suffers from a significant problem, since the exit pupil and eyebox have a trade-off relationship [12]. Kim and Park proposed a Maxwellian-type waveguide NED, which provides always focused images [13]. Magic Leap recently released a product that renders at two distinct focal planes [14].

In this Letter, we propose a dual-focal see-through waveguide-type NED using a novel combiner-eyepiece for AR. A novel optical device which is called a polarization-dependent lens device (PDLD) can support two different focal planes (near and infinity), depending on the polarization state of the input beam. The PDLD is an ultra-thin optical component based on a geometric phase holographic lens (GPHL) [15]. The proposed system with a compact form-factor can support near-correct focus cues for virtual images by controlling the polarization state of the display system.

The commercialized GPHL used in our proposed configuration is formed with polymerized liquid crystal, which has conjugation functions as a lens, depending on the polarization state. With left-handed circular polarized beams, the GPHL operates as a concave lens that has a negative focal length.
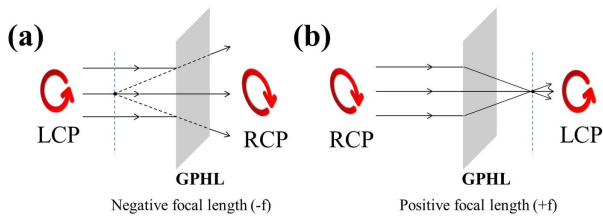
Fig. 1. Illustration of GPHL operation (a) with a left-handed circular polarization (concave lens) and (b) with a right-handed circular polarization (convex lens).

Fig. 3. Examination of dual-focal functionality using the PDLD: (a) experimental setup, (b) the captured image in optical window mode, and (c) the captured image in lens mode.

For right-handed circular polarized beams, they are converged at the focal point as shown in Fig. 1.

Figure 2 shows the schematic diagram of the PDLD which can operate in a lens mode or optical window mode. The PDLD consists of two GPHLs with same focal length, a quarter-wave plate (QWP) and a left-handed circular polarizer (LHCP). For the dual-focal plane, two GPHLs are stacked across the circular polarizer. The QWP attached on the front GPHL is used to convert the linearly polarized input beam into circular polarization, and the LHCP allows the rear GPHL to act as a concave lens, regardless of a polarization state of an input beam.

For a lens mode, a vertical polarized (i.e., s-pol) beam is incident on the PDLD; two GPHLs can act as a diverging lens in succession. In this case, the optical power of the PDLD is equivalent to half of the GPHL, because the circular polarizer film is very thin compared to the focal length. For an optical window mode, a horizontal polarized (i.e., p-pol) beam is incident on the PDLD; the functions of the two GPHLs cancel out each other, and the input beam can go through the PDLD without any further refraction. Because of the multi-functionality depending on the polarization state, it can be a suitable eyepiece lens for AR system [16,17]. The proposed optical device can be placed directly in front of the eye and be easily attached to the waveguide without any burdensome increase in form-factor by virtue of its flatness and thinness. Such a combiner-eyepiece similar to our proposed concept is of the design proposed in Ref. [18]. This combiner operates as a convex lens in the lens mode, which is unsuitable for waveguide systems.

In Fig. 3, multi-functionality of the proposed device by changing a polarization state of the input beam is demonstrated. To verify the feasibility, we captured changes in the size of the beam while changing the distance of the screen.
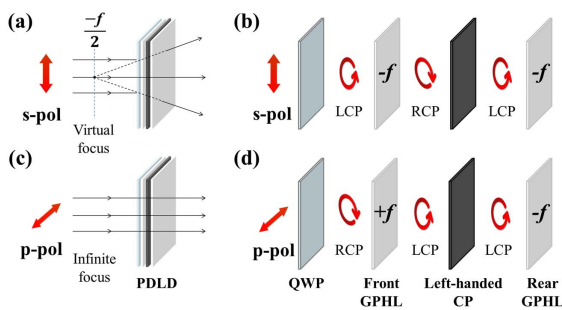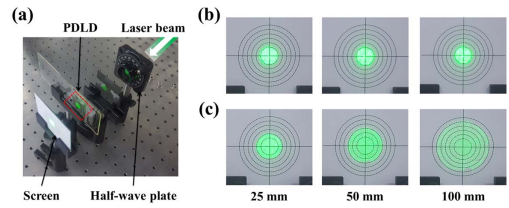
The radius of the output beam does not change with an s-polarized collimated beam. On the other hand, as the distance of the screen from the PDLD increases, the p-polarized beam diverges. These results are well matched with the configuration of the scheme in Fig. 2.

The two-dimensional schematic diagram of proposed waveguide-type NED with a PDLD is shown in Fig. 4. The system consists of a laser scanning projector (LSP), a polarization rotator unit, a planar waveguide, reflection-type volume holographic gratings (VHGs), a linear polarizer, and a PDLD.

The randomly polarized light emitted from the LSP is converted to a linear polarization state by a polarization rotator unit, which can support time-sequential polarization multiplexing. The linearly polarized beam is incident on the waveguide and diffracted by the in-coupler VHG. The diffracted beam propagates along the waveguide by total internal reflection; then the extracted beam by the out-coupler VHG enters the PDLD. By synchronizing a polarization rotator and an LSP, the proposed system can support two discrete focal planes that are located at infinity or near distance according to the optical power of the PDLD. Instead of micro-display and collimating optics, the LSP is adopted to render virtual images. This projection-based display has several advantages for a compact display module such as enough contrast and brightness in ambient light. In order to enlarge a limited exit pupil caused by the narrow beam waist of the laser, the system is designed with exit pupil expander (EPE) [19]. The in-coupler and out-coupler VHGs are fabricated with photopolymer holographic optical elements (HOEs). The recorded HOE only diffracts the input beam within a specific bandwidth of incidence angles, which can be interpreted as angular selectivity based on a coupled
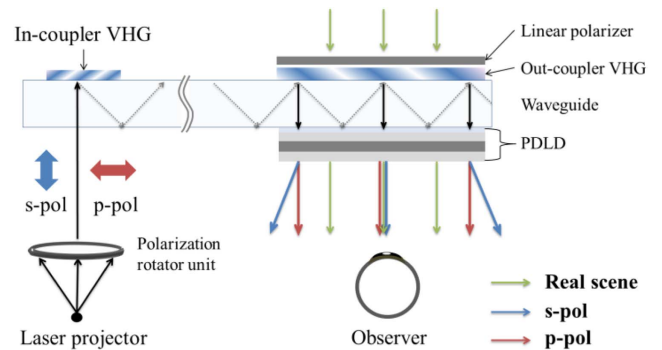

Fig. 2. Illustration of the proposed structure of the PDLD and the polarization state (a) in the lens mode and (b) in the optical window mode.

Fig. 4. Schematic diagram of proposed see-through waveguide-type NED system. The green lines indicate the ray from the real scene. The blue and red lines indicate the optical paths of light emitted by a display system with a polarization rotation device.
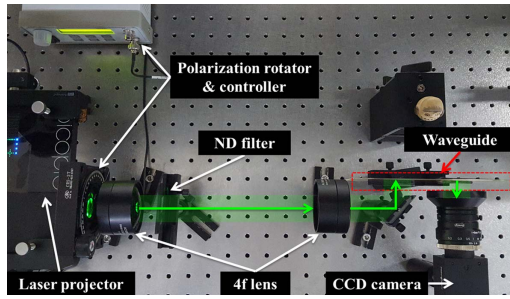
Fig. 5. Experimental setup of proposed configuration on an optical table. The green arrow indicates the path of light.

wave theory (CWT) [20]. To observe a real scene without distortion, the horizontal polarizer is located in front of the out-coupler. In this case, a see-through real-world scene can be observed. The air gap between the polarizer and out-coupler has to be taken into the consideration in the EPE scheme and is 0.1 mm in our experiment.

The experimental setup for the waveguide-type AR NED system was constructed on an optical table. The corresponding prototype is shown as Fig. 5. The commercialized LSP (VPL-201) is used in the experiment. The display resolution is 960×540 pixels, and the maximum optical scanning angle is 43° in horizontal direction. The clear aperture of the polarization rotator is 25.4 mm, which acts as an entrance stop that limits the overall range of projection angle. This limited value is 35° and is larger than the angular selectivity of the recorded HOE, which can guarantee field of view (FOV) of 10.5° in full-width at half-maximum (FWHM) along the horizontal direction. A 4-f lens system is set up to focus the input beam on the in-coupler HOE. The focal lengths of the two lenses that construct the 4-f optical system are 75 and 150 mm, respectively. The optical couplers are recorded with a wavelength of 532 nm. The planar waveguide is produced using a polished glass of which thickness is 0.6 mm. The focal length of the GPHL is 100 mm, and the thickness is 0.45 mm. The total thickness of the PDLD is about 1.5 mm, the effective focal length is −50.1 mm in the lens mode, and the transmission efficiency is about 46% for a randomly polarized beam when measured.

Figure 6 demonstrates the limiting factors of the FOV in the proposed configuration. First, the size of an exit pupil is equal to the width of the PDLD. The FOV θ_1 limited by the PDLD can be simply written as

$$\theta_1 = 2 \arctan\left(\frac{g}{2r}\right), \qquad (1)$$

where g is the size of the PDLD, and r is the eye relief. In our experiment, g is 25.4 mm, and r is set to 20 mm, which provide a 64.8° FOV at maximum. A wide viewing angle can be achieved due to the close distance of the eyepiece lens. Secondly, when the PDLD operates as an optical window, the FOV θ_2 limited by the out-coupler HOE is determined by the angular selectivity of the VHG, which is 10.5° on the FWHM criterion. Thirdly, in the lens mode, the distance of a virtual image plane has a repercussion on the FOV, which can be given as

$$\theta_3 = 2 \arctan\left[\frac{f \tan(\theta_2/2)}{f + r}\right], \qquad (2)$$

where f is an absolute value of the focal length of the PDLD. By applying the optical specification in our experiment, the calculated FOV is 7.5°. Finally, the FOV is limited by the lowest limit of the three cases mentioned above, and the display system provides up to 7.5° of monocular FOV along the longitudinal axis. The narrow viewing angle can be resolved by the improved design of the VHG [21]. The size of the retinal image also depends on the operating mode of the PDLD. The ratio of the retinal image size m can be easily derived in the same way as the FOV, which is given as

$$m = \frac{S_{\text{inf}}}{S_{\text{lens}}} = 1 + \frac{r}{f}, \qquad (3)$$

where S_{inf} is the size of the retinal image on the optical window mode, and S_{lens} is the size of the retinal image on the lens mode. Both the FOV and the ratio of image size are sharply converged, as the focal length of the PDLD becomes longer. By using the PDLD with a focal length greater than 180 mm, the difference between the two modes is less than 10%, as shown in the dotted lines of Figs. 6(d) and 6(e). Since the retinal image size is related to angular resolution, this difference for the operating mode should be small to form a uniform resolution within them.

The brightness of the virtual image highly depends on the operating mode of the PDLD. The diffraction efficiency for each polarization state can be calculated based on the CWT, as shown in Fig. 7. The output value is normalized by the result of s-polarization. The optical efficiency of lens mode is about 2.5 times higher than that of a see-through mode. For uniform brightness on two modes, an active display module interlocking with the polarizing rotator can be one solution. In our experiment, the brightness difference is compensated for by adjusting the brightness of the original input image.

Figure 8 shows the photographs of the experimental results taken with different focal planes of a CCD camera, which is located at the distance of eye relief with an exposure of 0.1 s. A camera lens has $f/1.4$ and 8 mm focal length. The aperture diameter of the lens is similar to the pupil size of the human eye in a normal environment. To visualize the change of focal distance, a woman-shaped toy is placed at 20 diopters (near),
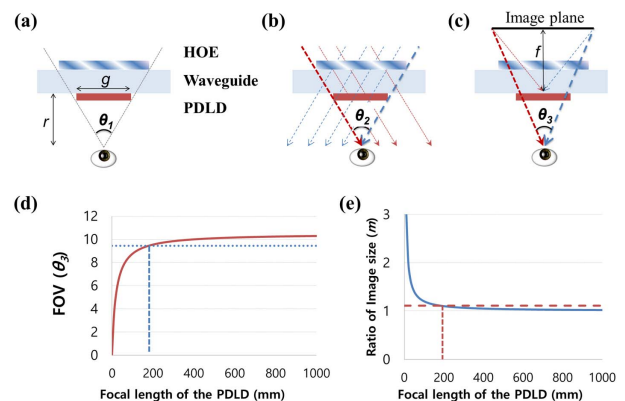

Fig. 6. Schematic diagram of FOV limitation (a) by the size of the PDLD, (b) by the angular selectivity of the HOE in the optical window mode, and (c) in the lens mode. (d) Relationship between the FOV in the lens mode and the effective focal length of the PDLD. (e) Relationship between the ratio of the retinal image size and the effective focal length of the PDLD.
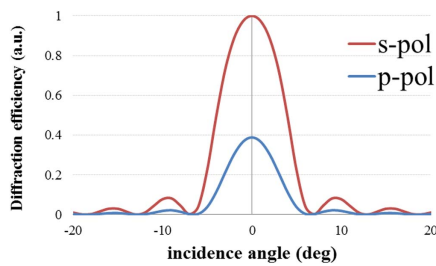
Fig. 7. Diffraction efficiency of the HOE with different polarization states.
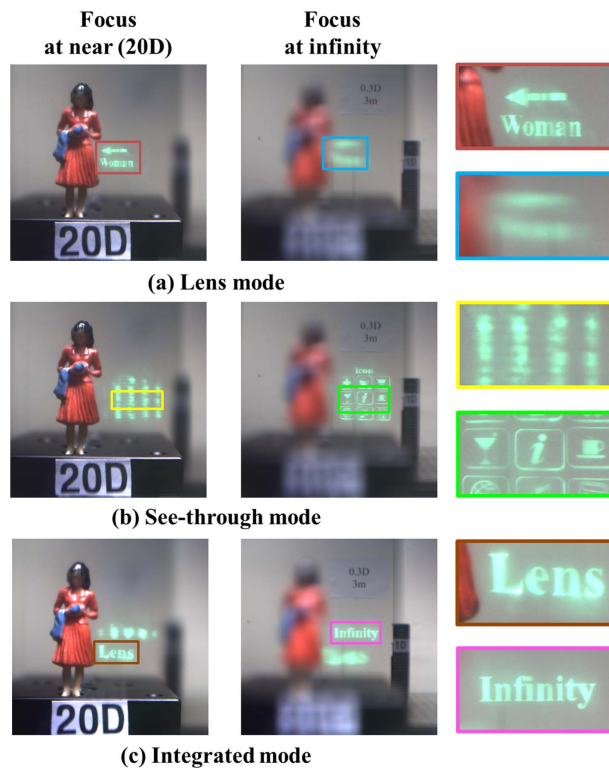

Fig. 8. Photographs of experimental results: (a) in the lens mode, (b) in the optical window mode, and (c) in the integrated mode.

a bar-type target is placed at 1 diopter (middle), and a white wall is located at 0.3 diopter (far). Virtual objects, texts, and a logo are rendered at 20 and zero diopters, respectively according to the operating mode of the PDLD. In the lens mode, the virtual image is sharply focused when the camera focuses at 20 diopters, as shown in Fig. 8(a). Figure 8(b) shows the see-through mode, when the virtual image is rendered at infinity. In this case, virtual images are blurred when the camera focuses at the woman toy (near object), and the blurred shape is determined by the replicated exit pupils by the EPE. When the camera focuses on the text on the paper attached to the wall (far object), the logo (virtual image) is in focus. In Fig. 8(c), both virtual images placed near and at infinity are simultaneously visualized by synchronization with the polarization rotator.

If the contents of the near and far images are overlapped, proper occlusion cues should be considered by using a depth-map filtering algorithm [22].

In the prototype setup, the virtual images have non-uniform brightness and slight distortion. These issues may arise from local defects of the HOE and misalignment of optics in the recording setup. The PDLD used in the experiment has a very short focal length for the eyepiece lens. For practical use, the virtual image should be rendered at practical near-field which is near arm reach [23]. This suitable distance can be achieved with a longer focal length of the GPHL.

In this Letter, we have proposed a waveguide see-through NED configuration with a dual-focal plane using a PDLD, which can selectively refract the incident light depending on the polarization state. This property is suited for eyepiece lenses for AR devices. The proposed method enables a dual-focal plane display with a compact form-factor. We have demonstrated a proof-of-concept system in which focal distances are located at infinity and 20 diopters, respectively. It can be expected that our proposed system can improve the sharpness of virtual images superimposed on real objects and mitigate the visual fatigue by the VAC problem.

REFERENCES

1. B. C. Kress and W. J. Cummings, SID Int. Symp. Digest Tech. Papers **48**, 127 (2017).
2. M. J. Heinrich and M. I. Olsson, "Wearable display device," U.S. patent D659,741 (May 15, 2012).
3. H. Mukawa, K. Akutsu, I. Matsumura, S. Nakano, T. Yoshida, M. Kuwahara, and K. Aiki, J. Soc. Inf. Disp. **17**, 185 (2009).
4. K. Sarayeddine and K. Mirza, Proc. SPIE **8720**, 87200D (2013).
5. T. Caudell and D. Mizell, *Proceedings of Hawaii International Conferences on Systems Sciences* (Hawaii, 1992), pp. 659–669.
6. T. Shibata, J. Kim, D. M. Hoffman, and M. S. Banks, J. Vis. **11**(8):11, 11 (2011).
7. S. Liu and H. Hua, Opt. Lett. **34**, 1642 (2009).
8. D. Kim, S. Lee, S. Moon, J. Cho, Y. Jo, and B. Lee, Opt. Express **26**, 17170 (2018).
9. N. Matsuda, A. Fix, and D. Lanman, ACM Trans. Graph. **36**, 1 (2017).
10. T. Zhan, Y. H. Lee, and S. T. Wu, Opt. Express **26**, 4863 (2018).
11. H. J. Yeom, H. J. Kim, S. B. Kim, H. Zhang, B. Li, Y. M. Ji, S. H. Kim, and J. H. Park, Opt. Express **23**, 32025 (2015).
12. A. Maimone, A. Georgiou, and J. S. Kollin, ACM Trans. Graph. **36**, 1 (2017).
13. S.-B. Kim and J.-H. Park, Opt. Lett. **43**, 85 (2018).
14. I. Hamilton, "What magic leap one and Facebook's half dome have in common," 2015, https://uploadvr.com/magic-leap-one-half-dome-common-differences.
15. J. Kim, Y. Li, M. N. Miskiewicz, C. Oh, M. W. Kudenov, and M. J. Escuti, Optica **2**, 958 (2015).
16. J.-Y. Hong, C.-K. Lee, S. Lee, B. Lee, D. Yoo, C. Jang, J. Kim, J. Jeong, and B. Lee, Sci. Rep. **7**, 2753 (2017).
17. G.-Y. Lee, J.-Y. Hong, S. Hwang, S. Moon, H. Kang, S. Jeon, H. Kim, J.-H. Jeong, and B. Lee, Nat. Commun. **9**, 4562 (2018).
18. C.-K. Lee, et al., *International Display Workshops* (The Society for Information Display, 2018), pp. 758–761.
19. P. Äyräs, P. Saarikko, and T. Levola, J. Soc. Inf. Disp. **17**, 659 (2009).
20. H. Kogelnik, Bell Syst. Tech. J. **48**, 2909 (1969).
21. J. Han, J. Liu, X. Yao, and Y. Wang, Opt. Express **23**, 3534 (2015).
22. R. Narain, R. A. Albert, A. Bulbul, G. J. Ward, M. S. Banks, and J. F. O'Brien, ACM Trans. Graph. **34**, 59 (2015).
23. P. E. Napieralski, B. M. Altenhoff, J. W. Bertrand, L. O. Long, S. V. Babu, C. C. Pagano, J. Kern, and T. A. Davis, ACM Trans. Appl. Percept. **8**, 1 (2011).